ESA STUDY CONTRACT REPORT			
ESA Contract No 4000120250/17/NL/BJ	SUBJECT: Large Area high-performance Optical Filter for X-ray instrumentation (LAOF)		CONTRACTOR: AMETEK Finland Oy (ex. HS Foils Oy)
ESA CR ( ) No	DATE 21.10.2020	No of volumes 1/1	Contractor's Reference LAOF-TN-10, Issue 3

Technical Note 10 – Filter Characterization Report

Corresponding Work Package 4: Target filter test

ABSTRACT

This document describes the main results obtained from characterization measurements performed on different filter samples designed and manufactured within this contract. Thin films of silicon nitride and polyimide of different sizes (ranging from 10 to 100 mm), shape (circular or square) and mechanical design (e.g. meshless or supported by Si or polyimide meshes) have been manufactured within this contract to investigate new solutions to build optical blocking filters for X-ray detectors in future space applications. In addition, preliminary measurements have been performed on a new material based on CNT which will be further investigated in a CCN of this contract.

The characterization measurements, obtained with a suite of different techniques, provide very useful results for future developments of the investigated materials.

The work described in this report was done under ESA Contract. Responsibility for the contents resides in the authors or organization that prepared it.

Authors:

Marco Barbera, UNIPA, Palermo, Italy
Luisa Sciortino, UNIPA, Palermo, Italy
Pekka Törmä, AMETEK Finland Oy

Contributors:

Ugo Lo Cicero, Salvatore Varisco, Fabio D'Anca, INAF-OAPA, Palermo, Italy
Elena Puccio, Michela Todaro, Salvatore Ferruggia Bonura, UNIPA, Palermo, Italy
Nicola Montinaro, UNIGE, Université de Genève, Switzerland

NAME OF ESA STUDY MANAGER DIV: DIRECTORATE:	ESA BUDGET HEADING

Project: Large area high-performance optical filter for X-ray instrumentation	**Document:** Filter Characterization Report	Document Code: LAOF-TN-10

CONTENTS

1. Introduction

The main goal of the contract is the investigation of new filter materials for future high-energy astrophysics missions and in particular for the large ESA mission Athena, aiming at developing a European expertise in a field largely dominated by US manufacturers.

Different tests have been performed on small size samples and partially representative medium size filters manufactured by AMETEK Finland (Prime contractor) and OXFORD Inst. Finland in order to investigate material optical and mechanical properties, to constraint model parameters, to support the design optimization, and to verify the compliance to the requirements specified in the Statement of Work (Appendix 1 to ITT AO/1-8786 /16/NL/BJ) of this contract. This technical note reports the main results of filter characterization.

This document is the final version delivered at the end of the project when all characterization activities have been essentially concluded. The recent Covid-19 pandemic has partially affected the contract activities in the last 8 months, in particular, experimental activities have been significantly delayed due to lock-down of local and external facilities. Not all the characterization tests have been fully completed as desired, however, we consider the obtained results a complete suite well sufficient for the verification of the filter requirements defined in the contract SoW.

The experiments section is organized in several paragraphs, each of them describes a different characterization technique(s) and/or a specific treatment.

2. Requirement and Characterization Matrix

In the Statement of Work (SoW) of the project a large number of requirements and specifications for the manufactured filters are defined. These requirements are listed in table 1. Table 1 lists the characterization tests defined in the SoW. The verification column in both tables indicates the verification methods to be used, D stands for “by Design” and T stands for “by Test”.

Table 1: Requirement matrix of the filters defined in the Statement of Work.

Req.	Parameters	Specification	Comments	Verif.
Req-1	Effective area	Large: 185x185mm2 TBC Medium: Ø 50mm Small: Ø 25mm	WFI requires filters of 165x165 mm² to 185x185 mm² size, depending on filter wheel design. The medium and small filters are representative for the XIFU need and have to operate at cryogenic temperature.	D
Req-2	Open area	90%	The support structure area shall be limited to 10%.	D
Req-3	Transmittance	68%@277ev 94%@1keV 98%@10keV	As compatible with instrument QE requirement breakdown.	D, T

Req-4	X-ray transmission uniformity	TBD	To be measured at Bessy facilities	T
Req-5	Material choice	Si, Al, O, N, C, H	Materials containing elements not on the list below shall only be used after discussion and approval by the customer. Filter is not shielded by WFI graded Z shield. Use of high-Z materials (e.g. stainless steel or Ti wire meshes) leads to increased background due to X-ray fluorescence.	D
Req-6	Visible/IR rejection	10^{-2}	Values taken from instrument internal science requirements breakdown as presented by instrument consortium filter groups. Drivers are: UV: Optical loading in WFI (observations of bright O-B stars) VIS – FIR: thermal and optical load on X-IFU	D, T
Req-7	Operation Temperature	Large filter: 253K – 320K Medium filter: 10K – 320K Small filter: 1K – 320K	WFI filter and outer X-IFU filters are operated at ambient conditions. Inner filters of X-IFU operate at cryogenic temperatures down to sub-Kelvin. High temperature limit set near 50C to allow decontamination heaters if needed.	D, T
Req-8	Storage temperature	25+/- 5 °C		
Req-9	Mount compatibility	Mounting shall be contiguous metallic, conductive, light tight	EMC/stray-light protection	
Req-10	Maximum weight	100g (TBC)	Including the mount	D
Req-11	Unique labelling		A unique and permanent serial number must be attributed to each filter. This is part of the PA plan to ensure the traceability of each manufacturing steps for each filter	
Req-12	Marking notch		The notch shall be used as reference in order to identify the exact rotation of the matrix	

Table 2: Characterization matrix for the filters defined in the Statement of Work.

<table>
<tr><th>Req.</th><th>Parameters</th><th>Specification</th><th>Comments</th><th>Verif.</th></tr>
<tr><td>Req-13</td><td>Thermal cycling</td><td>Total Number of cycles : 100

thermal cycles, from 293K to 100K (small/medium) or 320 to 253K (large), dwell time >20 minutes, slope <3K/minute</td><td>See AD2</td><td>D, T</td></tr>
<tr><td>Req-14</td><td>Vibration</td><td>Sine (5-100Hz): 25g

Random:

axial/lateral QUAL
f1 [Hz] f2 [Hz] PSD
20 100 3.00 dB/oct
100 300 0.50 g^2/Hz
400 2000 -5.00 dB/oct</td><td>25g DLL as worst case, Athena instruments parameters</td><td></td></tr>
<tr><td>Req-15</td><td>Acoustic load</td><td><table><tr><th>Octave centre frequency [Hz]</th><th>Limit level [db] (reference: odb = 2e-5 Pa)</th></tr><tr><td>31.5</td><td>128</td></tr><tr><td>63</td><td>131</td></tr><tr><td>125</td><td>136</td></tr><tr><td>250</td><td>133</td></tr><tr><td>500</td><td>129</td></tr><tr><td>1000</td><td>123</td></tr><tr><td>2000</td><td>116</td></tr><tr><td>OASPL (20-2828Hz)</td><td>139.5</td></tr></table></td><td>Acoustic noise spectrum under fairing of Ariane 5, taken from A5 user's manual.</td><td>T</td></tr>
<tr><td>Req-16</td><td>Radiation</td><td>Total ionising dose: 50kRad Non-ionising Energy loss: 9.4x10^{+10} #/cm^2 (Eq 10 MeV Proton Fluence)</td><td>Assumes 1 mm Aluminium shielding on the Athena spacecraft</td><td>T</td></tr>
<tr><td>Req-17</td><td>Shock level</td><td>axial/lateral Q=10 QUAL
f [Hz] SRS [g]
100 20
1000 400
10000 400</td><td>From Athena Instrument requirements</td><td>T</td></tr>
<tr><td>Req-18</td><td>Static overpressure</td><td>0.05 bar Large Filters

0.1 bar for small filters (goal 1.2 bar)

(Amended to 6 mbar for the X-IFU filters, and 16 mbar for the WFI filters, see MOM of DDR meeting held in Helsinki on Feb. 21, 2018.)</td><td>A factor 2 shall apply to the filter in order to be considered successful. Instrument consortia currently assume 10mbar static overpressure. This seems optimistic.</td><td>T</td></tr>
</table>

Req-19	Pin hole	The pinhole area shall be less than $2x10^{-7}$ mm^2 / cm^2	best value achieved for XMM	T
Req-20	Moisture stress	Humidity < 70% at 25+/- 5 °C	Driven by the humidity under the fairing	T

3. Samples Description

All the filter samples manufactured by the main contractor and sub-contractors delivered to UNIPA are reported in the table enclosed in the ANNEX1. The table includes the main characteristics of the filter samples and identifies the type of characterization measurements performed. Small size filters have been mounted on aluminum round frames according to the TO8 SCHOTT standard (ANNEX2), LUXEL standards TF110 (ANNEX 3), TF111 (ANNEX4), TF112 (ANNEX5), while manufactured medium size filters have been mounted on custom frames designed by UNIPA, namely D56 (ANNEX6), and LDA WFI single quadrant (ANNEX7), finally large size filters have been mounted on custom two parts type frames designed by UNIPA (ANNEX8).

Medium and large size filters under test are categorized with respect to the material type as follows:

Si_3N_4 + Si Mesh Samples

Medium size filters of Si_3N_4 supported by Si meshes have been manufactured by AMETEK Finland and have been mounted on two parts type frames TF112 according to LUXEL standards (ANNEX5). The frame (figure 1) has the following dimensions

- outer frame outer diameter: 51.3 mm
- outer frame clean aperture: 38.1 mm
- inner frame outer diameter: 43.0 mm
- inner frame clean aperture: 39.7 mm

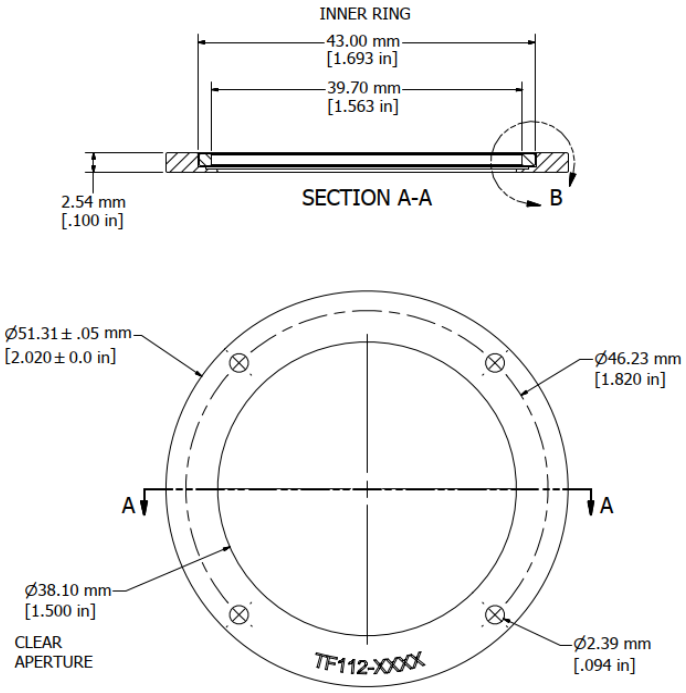

Fig. 1 – TF112 standard LUXEL circular frame.

The full set of filters of this type delivered to UNIPA and their characteristics are listed in ANNEX 1.

Polyimide + Polyimide Mesh Samples

Medium size filters of polyimide supported by polyimide meshes have been manufactured by OXFORD Instruments, Finland and have been mounted on two parts type frames designed by UNIPA (figure 2) and manufactured by HS-FOILS according to the executive drawing in ANNEX7. The frame, which corresponds to a single quadrant of the optical blocking filter designed for the Athena Wide Field Imager - Large Detector Array has the following dimensions

- outer dimensions: 120 x 120 mm
- clean aperture: 82 x 82 mm
- inner frame outer dimensions: 94 x 94 mm
- inner frame clean aperture: 82 x 82 mm

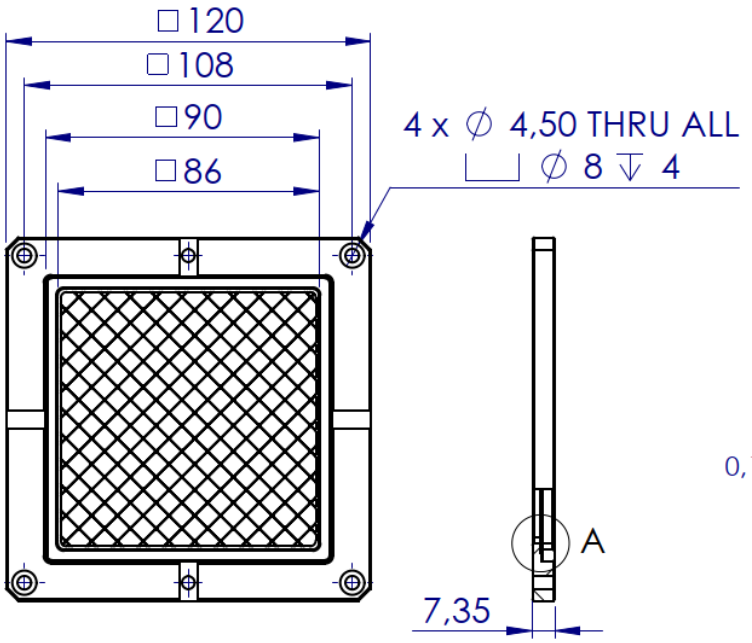

Fig. 2 – Custom frame of a single quadrant Athena WFI Large Detector Array optical blocking filter.

A large size filter of polyimide supported by polyimide meshes has been manufactured by OXFORD Instruments, Finland and has been mounted on two parts type frames designed by UNIPA (figure 3) and manufactured by HS-FOILS according to the executive drawing in ANNEX8.

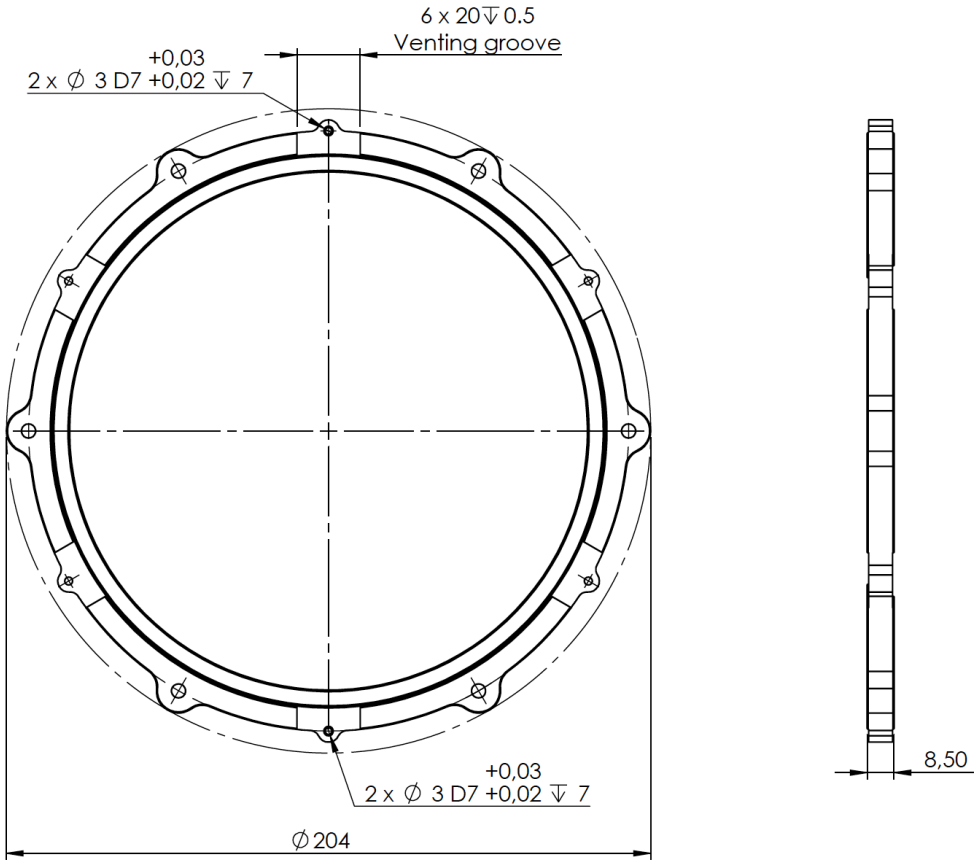

Fig. 3 – Custom frame of a X-IFU filter wheel optical blocking filter.

The full set of filters of this type delivered to UNIPA and their characteristics are listed in ANNEX 1.

CNT (Carbon Nano Tubes) Samples

Medium size filters of meshless CNT pellicles have been procured by AMETEK Finland and have been mounted on two parts type frames designed by UNIPA and manufactured by HS-FOILS according to the executive drawings in in ANNEX6 (preliminary model of an intermediate size ATHENA X-IFU thermal filter) and ANNEX7 (WFI LDA single quadrant optical blocking filter). The filter in ANNEX6 (figure 4) has the following dimensions

- outer frame outer diameter: 82.0 mm
- outer frame clean aperture: 56.0 mm
- inner frame outer diameter: 66.0 mm
- inner frame clean aperture: 58.0 mm

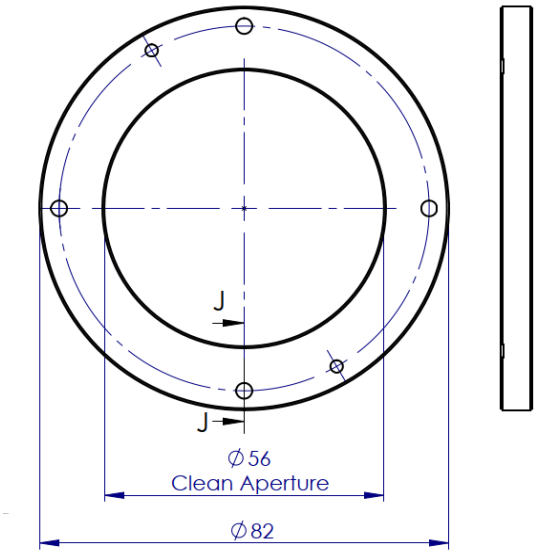

Fig. 4 – Custom frame of a preliminary model of an intermediate size ATHENA X-IFU thermal filter.

The full set of filters of this type delivered to UNIPA and their characteristics are listed in ANNEX 1.

4. Visual Inspection

The main goal of this characterization activity is to identify and map defects on the full area of the filters. Track location and morphology of major pinholes and defects to get feedback on the production processes and to investigate evolution after environmental tests and radiation damage tests. The characterization procedure includes a filter scan when we get the filter for the first time, and other scans after every test that may cause changes on the filter. Scanner images of all filters delivered to UNIPA by AMETEK have been taken in reflectivity mode and transmissivity mode using the optical photographic scanner (EPSON Perfection V850 Pro model). The following figures 5 and 6 show as an example the scanner images of the W3a-#01 Poly-Poly mesh filter sample. In the second image (transmissivity mode) some dust particles (red circles) and pin holes (yellow circle) identified by analyzing the images are marked.

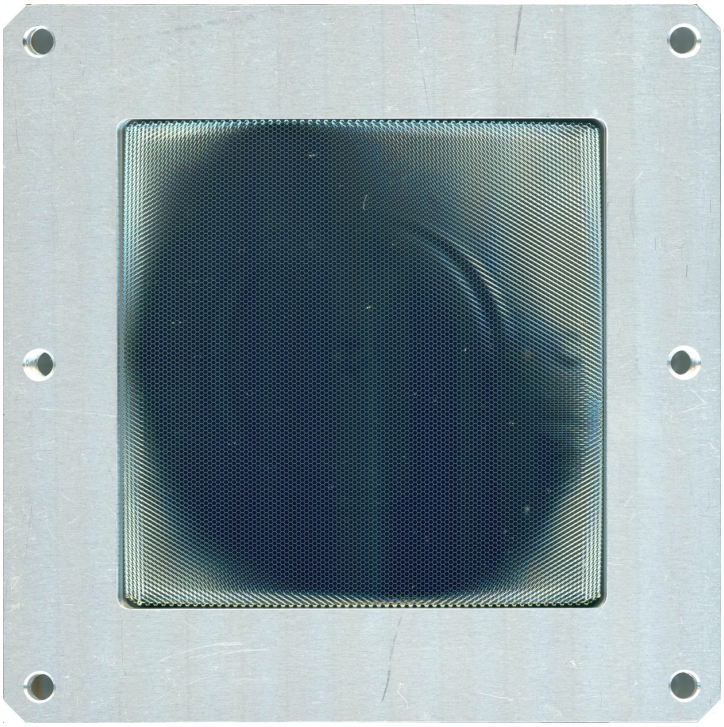

Fig. 5 – Optical scanner image taken in reflection mode of the W3a-#01 sample.

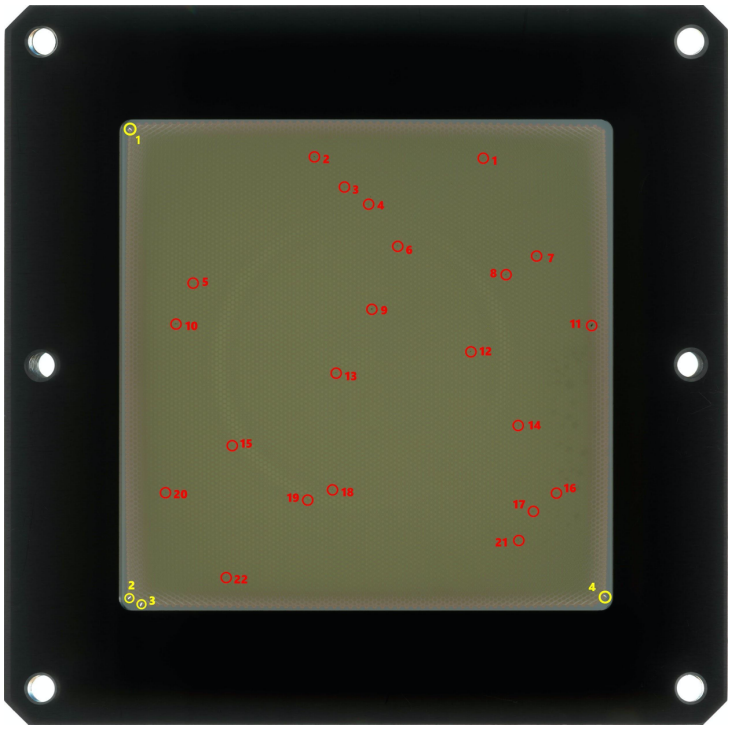

Fig. 6 – Optical scanner image taken in transmission mode of the W3a-#01 sample. The largest specks of dust are highlighted with red circles and the four identified pinholes with yellow circles.

A detailed analysis of each image is a very time consuming activity and has been performed only on few samples. The full set of scanner images and inspection notes on medium and large size filters will be organized in a proper repository and uploaded onto the project cloud before the final review of the contract.

5. Proton Irradiation

The main goal of this activity is to verify radiation hardness of filters to doses comparable to those of a lifetime in Space. Two different types of filters have been irradiated by 1 MeV protons with different fluences, according to table 3, at the Van der Graaf accelerator at the Johann Wolfgang Goethe-Universität Frankfurt am Main. The main characteristics of the irradiation facility are given in TN9.

Table 3: Irradiated filters and fluences relative to the qualification fluence (QF).

0.1 x QF(1)	1 x QF	10 x QF	100 x QF	300 x QF
TO8 C2-4 TO8 C3-12	TO8 C2-5 TO8 C3-13	TO8 C2-2 TO8 C3-10	TO8 C2-3 TO8 C3-16	TO8 C2-7 TO8 C3-15

(1) QF = $1.2*10^{10}$ cm^{-2} @ 1 MeV

The main characteristics of the irradiated samples are reported in the ANNEX1 and here summarized:

- TO8 C2 series – 15 nm Al/40nm Si_3N_4 /15 nm Al
- TO8 C3 series - 10 nm Al/20nm Si_3N_4 /10 nm Al

The effect of particle irradiation on Si_3N_4 filters has been evaluated by Atomic Force Microscopy, X-ray Photoelectron Spectroscopy, Optical (UV-VIS-IR) Spectroscopy. The results are reported in the following sections SURFACE ANALYSIS and UV/VIS/NIR TRANSMISSION MEASUREMENTS.

6. Surface Analysis

A layer of aluminum oxide, nearly transparent in the UV/VIS, builds up on each surface. Determining the thickness of this layer is relevant to design the filter for maximum soft X-ray transmission and appropriate UV/VIS rejection. In addition, knowing the surface micro-roughness is relevant to establish the minimum thickness of the Al layer that provides adequate uniformity. We have used two techniques to investigate the surface of pristine and irradiated samples, namely: X-ray photoelectron spectroscopy to derive the amount of the aluminum oxide, and Atomic Force Microscopy to derive the surface roughness.

6.1 X-ray Photoelectron Spectroscopy

Al/SiN/Al samples

X-ray Photoelectron Spectroscopy (XPS) measurements were performed on two filter samples produced by AMETEK and made of silicon nitride and aluminum supported by a silicon mesh,

namely: TO8 C3-11 (pristine), and TO8 C3-16 (100 X QF irradiated).

The two filters consist of a thin silicon nitride layer of 20 nm, with a thin aluminum layer of 10 nm on both sides of the silicon nitride. A supporting Si mesh with a honeycomb pattern is present. Such a mesh is characterized by a bar height of 15 µm, bar width 18 µm, pitch size of 190 µm, and an overall open area (OA) of 81%. The TO8 C3-11 was measured pristine while the TO8 C3-16 was first irradiated with 10 MeV protons with a fluence of $1.26*10^{12}$ cm^{-2} corresponding to 100 x QF, and then measured with XPS.

XPS measurements were performed at the BACH beamline of the ELETTRA synchrotron (ELETTRA VUO proposal no. 20180369). The incident photon beam was at 60° with respect to the outgoing electrons. The sample was rotated 30° around the vertical axis with respect to normal incidence to optimize the signal revealed by the analyzer. The spot size of the beam was 300 µm x 50 µm (v x h).

For all the measurements, the available High Energy Undulator (175-1600 eV) at the beamline was used. Furthermore, we used two different gratings according to the different kinetic energies used, namely: SG2 (161-597 eV) and SG3 (490-1600 eV).

First, we calibrated the energies of the incident photon on a gold reference. Then, we performed XPS experiments with five different kinetic energies (KE) of the outgoing electron to probe different thickness of the sample, such a technique is known as depth profile. The selected kinetic energies and the respective probed thicknesses are: 100 eV (depth=1 nm), 200 eV (depth=1.3 nm), 490 eV (depth=2.1 nm), 800 eV (depth=3 nm) and 1020 eV (depth=3.6 nm). Since the aluminum oxide is always present on an aluminum surface, we acquired the XPS spectra of the Al 2p peak and of the O 1s peak for each KE for both samples. In this way, it is possible to estimate the amount of the native aluminum oxide and to compare the pristine and the irradiated samples.

The XPS measurements on Al 2p and O 1s peaks acquired at different KE on TO8 C3-16 filter sample are reported in fig. 7 and fig. 8.

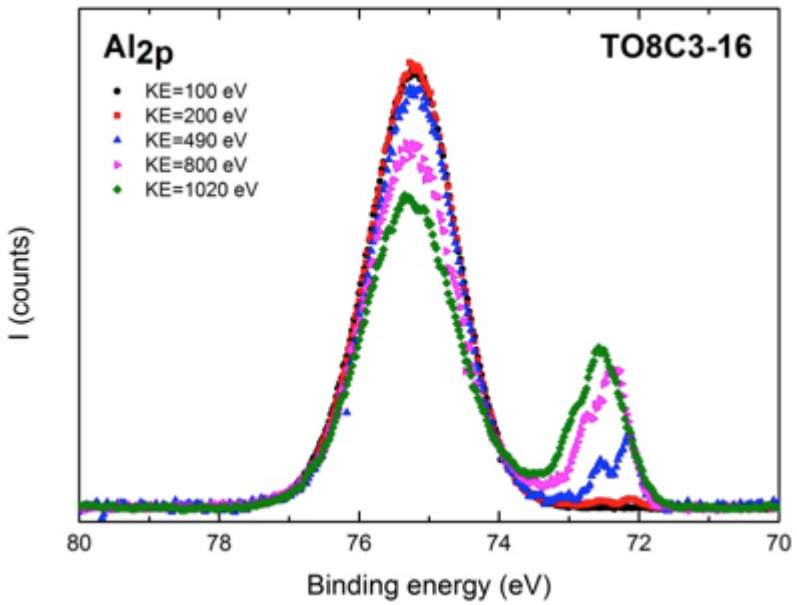

Fig. 7 – Normalized XPS measurements of the irradiated sample, the TO8C3-16 filter. The Al 2p peak acquired at different KE of the outgoing electron 100 eV (black), 200 eV (red), 490 eV (blue), 800 eV (magenta) and 1020 eV

(green). All spectra are normalized by the total area.

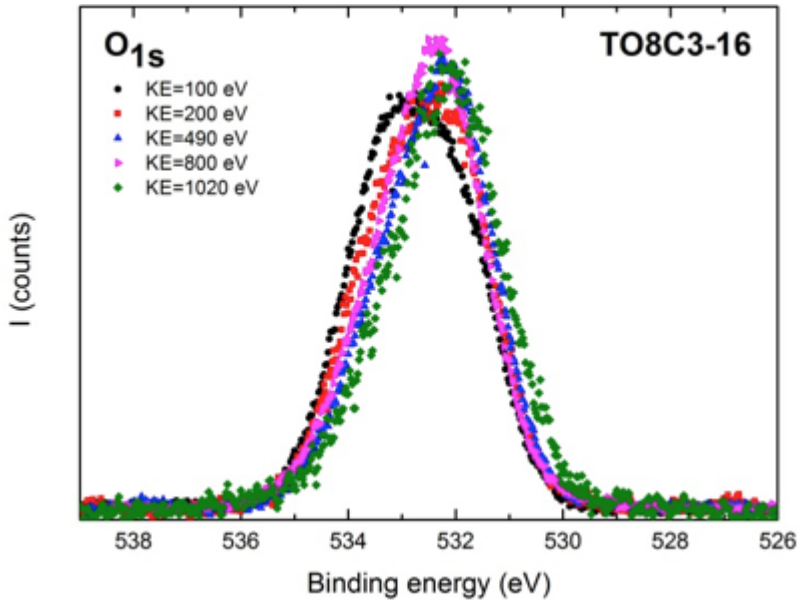

Fig. 8 – Normalized XPS measurements of the irradiated sample, the TO8-C3-16 filter. The O 1s peak acquired at different KE of the outgoing electron 100 eV (black), 200 eV (red), 490 eV (blue), 800 eV (magenta) and 1020 eV (green). All spectra are normalized by the total area.

The normalized Al 2p spectra are composed of two main signals: a major contribution at 75.3 eV binding energy (BE) attributed to the Al^{3+} component and a minor signal at about 73 eV assigned to Al^0 component. In particular, the signal assigned to metallic Al is doublet due to the spin-orbit coupling. This doublet corresponds to the two possible states having distinguishable binding energies, attributed to $2p_{1/2}$ and $2p_{3/2}$ Al peaks.

As the KE increases, the contribution of aluminum oxide decreases while the metallic aluminum component increases. In fact, as the KE increases, the thickness investigated by photons is greater, as a consequence, the ratio between thickness of revealed metallic aluminum and that one of superficial aluminum oxide increases.

All XPS spectra were analyzed by the "Peak analyzer" program of OriginPro 8.5.1. First, a baseline was subtracted, then the peaks were fitted using the Voigt functions. In particular, we used three Voigt functions for the Al 2p peak. Furthermore, the Full Width at Half Maximum of the Al^0 $2p_{1/2}$ and to the Al^0 $2p_{3/2}$ signals was constrained to be identical, and, for the same peaks, the ratio of the areas was constrained to be 1:2 as expected from theory. The goodness of the fit of Al 2p peak is shown in fig. 9, showing the Al^{3+} component and the two Al^0 components.

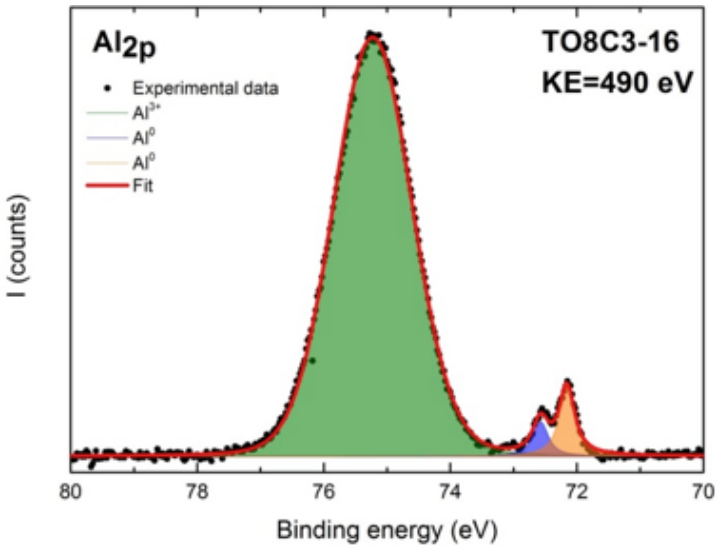

Fig. 9 – Fit for the Al 2p peak with KE of 490 eV of the irradiated sample TO8C3-16. Data reported are experimental (black full circle), best fit (red line), Al^{3+} 2p component (dark green filled curve), Al^0 $2p_{1/2}$ (blue filled curve), and Al^0 $2p_{3/2}$ (orange filled curve).

The normalized O 1s XPS spectra (fig. 8) are composed of a single signal. According to literature, this peak was analyzed as the combination of two components, one at about 532 eV BE, assigned to oxygen in Al_2O_3 layer and the other component at about 533.4 eV BE, related to the oxygen of the H_2O present on the sample surface. Despite the measurement condition of UHV (about 10^{-9} mbar typically), some water molecules were revealed on the filter surface.

The fit of all O 1s XPS spectra was performed as that described for Al 2p peak using only two Voigt functions. The two contributions of oxygen in H_2O and Al_2O_3 and best fit are shown in fig. 10.

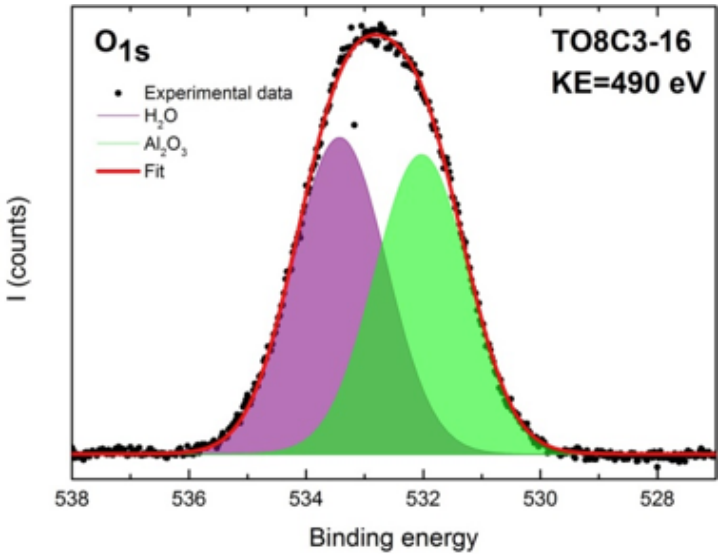

Fig. 10 – Fit for the O 1s peak with KE of 490 eV of the sample TO8-C3-16. Data reported are experimental (black full circle), best fit (red line), O of H_2O component (purple filled curve, and O of Al_2O_3 (green filled curve).

Starting from the analysis described above, the estimate of the aluminum oxide thickness is obtained by using the following equation:

$$d = \lambda o \, sin\theta \, ln(\frac{Nm \, \lambda m \, Io}{No \, \lambda o \, Im} + 1)$$

where d is the thickness of the oxide layer, λ_o and λ_m are the electron inelastic mean free paths (IMFP) in the oxide and the metal, respectively. θ is the electron take-off angle with respect to surface sample, N_o and N_m are the volume densities of the aluminum atoms in the oxide and the metal, respectively, and the I_o and I_m are the peak areas of the oxide and metal component of the Al 2p signal.

The plot of λ_o as a function of the inverse of the logarithm of the previous equation is reported in figure 11. Then according to the reported equation, the oxide thickness is calculated as the slope of the linear fit, that gives the thickness of Al_2O_3 equal to 4.0 nm 3.9 nm for the TO8-C3-11 and for the TO8-C3-16 samples, respectively.

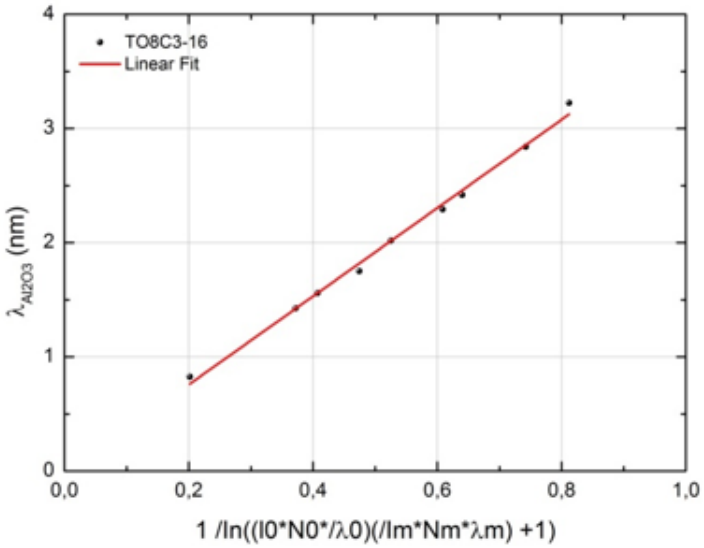

Fig. 11 – λ_o vs the inverse of the logarithm of the reported equation (black circles) and the best fit (red line).

Our analysis shows that the aluminum oxide thicknesses are essentially comparable for the pristine and the irradiated samples within the error. Therefore, we can conclude that even the higher fluence of irradiation has no effect on the thickness of the native oxide on the aluminum surface.

Al/CNT/Al samples

X-ray Photoelectron Spectroscopy (XPS) measurements were performed on a sample made of a carbon nanotubes pellicle provided by Ametek with no mesh, the LAOF-CNT2-C1B2-F02 (sample 14 nm Al/ 120-150 nm CNT/ 14 nm Al).

XPS measurements were performed at the BACH beamline of the ELETTRA synchrotron (ELETTRA VUO proposal no. 20190214). The incident photon beam was at 60° with respect to the outgoing electrons. The emission angle was set at 90°. The spot size of the beam was 300 µm x 50 µm (v x h).

For all the measurements, the available High Energy Undulator (175-1600 eV) and the SG3 grating (490-1600 eV) at the beamline were used.

First, we calibrated the energies of the incident photon on a gold reference and the adventitious carbon to take into account for the grating calibration and the potential charge effect. Then, we performed XPS experiments with three different kinetic energies (KE) of the outgoing electron to probe different thicknesses of the sample: 450 eV, 550 eV, and 750 eV.

Since the aluminum oxide is always present on an aluminum surface, we acquired the XPS spectra of the Al 2p peak and the O 1s peak for each KE for the aluminum-coated sample on one surface. In our hypothesis, the two aluminum surfaces are indistinguishable.

The gold 4f doublet was used to recover the real energy of the incident photon, which is 622.6 eV. After this procedure of calibration, the C1s peak is located at 284.5 eV that is in good agreement with the C 1s peak of the graphite at 284.4 reported by the NIST.

Then there is no energy shift due to charge effect, in other words, we can state that these samples are conductive. This property allows studying carefully such materials with the XPS techniques.

The measured counts are corrected for the real incident flux and for the non-linear response of the detector. In all analyses, a Shirley background has been subtracted from the raw data. The Al 2p peak recorded at three different kinetic energies 450, 550, and 750 eV is shown in fig.12.

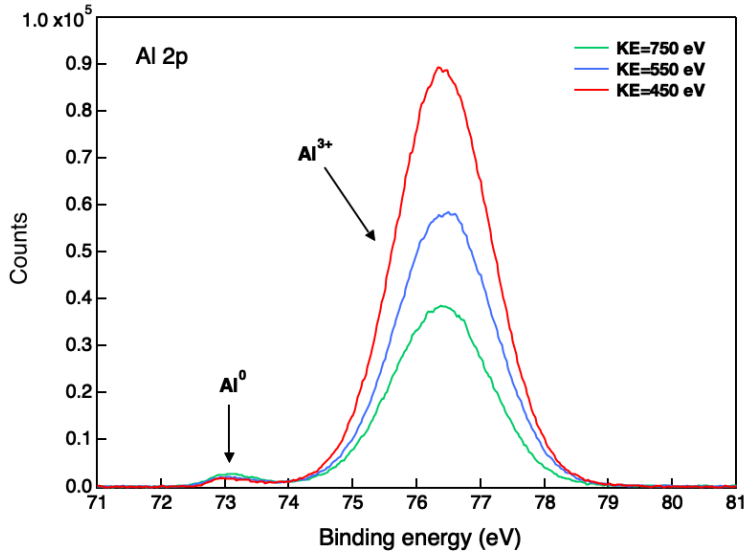

Fig. 12 – Al 2p peak for the sample LAOF-CNT2-C1B2-F02 (14 nm Al/ 120-150 nm CNT/14 nm Al) acquired at three different kinetic energies: green line 750 eV, blue line 550 eV, and red line 450 eV.

The O 1s peak recorded at the same three different kinetic energies, namely 450, 550, and 750 eV is shown in fig. 13.

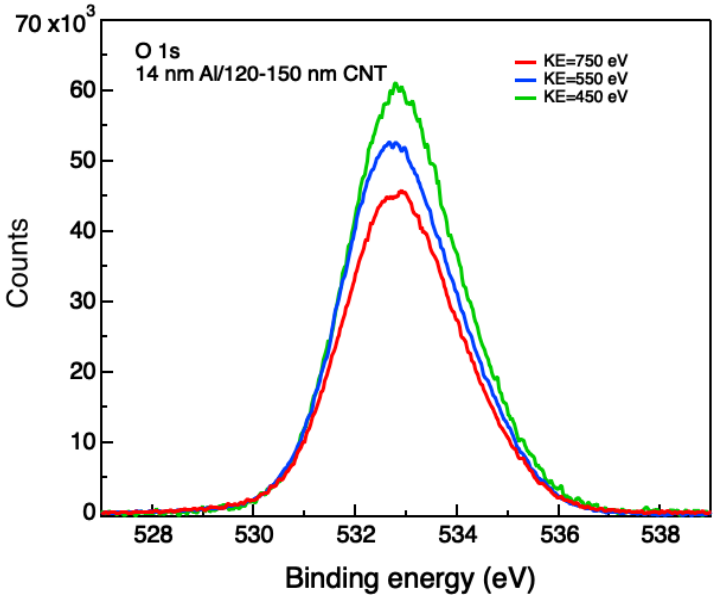

Fig. 13 – O 1s peak of the LAOF-CNT2-C1B2-F02 (14 nm Al/ 120-150 nm CNT/14 nm Al), at three different kinetic energies: green line 450 eV, blue line 550 eV, and red line 750 eV.

Two main components are recognizable in the Al 2p at two binding energies, 73 eV and 76.5 eV (fig. 12). The signal at 73 eV is ascribable to the presence of metallic aluminum, while the signal at higher energy is due to the presence of aluminum in the +3 oxidation state, in other words, this component points out the presence of aluminum oxide. Furthermore, the ratio of the areas of the signal highlights a large amount of oxide, that may be caused by the large specific area of the membrane (low density) that might facilitate the oxidation of the deposited aluminum.

Our preliminary data show that the amount of the aluminum oxide is higher than the metallic aluminum, therefore, a component of the O 1s peak in fig. 13 may be ascribable to the Al_2O_3. Furthermore, by comparing the Al 2p spectra of fig.8 at kinetic energy 490 eV to the peak at kinetic energy 450 eV in fig. 12 (red line) it is worth noting that the ratio between the areas of the two main signals at 73 eV and 76.5 eV is larger for the silicon nitride sample, thus pointing out a larger amount of aluminum oxide for the CNT sample.

The asymmetry of the O 1s peak suggests that there are at least two different components to the spectra reported in fig. 13. We hypothesize that the other component might be justified by the presence of water molecules.

6.2 Atomic Force Microscopy

Atomic Force Microscopy (AFM) measurements are acquired in air by using a Bruker FAST-SCAN microscope. The images are obtained in tapping mode by using FAST-SCAN probes with apical radius of about 5 nm. Each AFM image has a pixel resolution comparable to the tip size and surface micro-roughness down to ~ 5 nm. The roughness of the surface has been measured over large areas 8 μm x 8 μm.

Three different samples were measured as reported in table 4. Two of the measured samples are pristine, TO8-C2-1 and TO8-C2-6, and one has been irradiated, TO8-C2-3.

Table 4: List of investigated samples by AFM with the calculated roughness, the average height and the width of the height function distribution.

Sample	Irradiation level	Roughness [nm]	Average Height [nm]	Average Height distribution width [nm]
TO8-C2-1	Pristine	1.95	12.75	4.57
TO8-C2-6	Pristine	3.56	13.78	5.68
TO8-C2-3	100 QF	2.39	9.32	3.33

The acquired images were analyzed using the gwyddion data analysis software and are reported in figs. 14 a,b,c,d,e,f,g,h,i.

<table>
<tr><th colspan="2">PRISTINE</th><th>IRRADIATED 100 QF</th></tr>
<tr><th>TO8-C2-1</th><th>TO8-C2-6</th><th>TO8-C2-3</th></tr>
<tr><td> 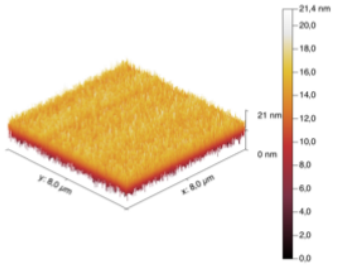
a) 3D AFM image of upper surface of the TO8-C2-1</td><td> 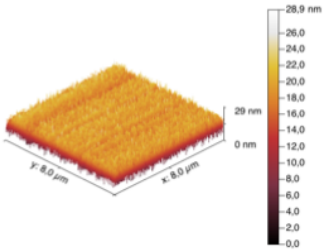
b) 3D AFM image of upper surface of the TO8-C2-6</td><td> 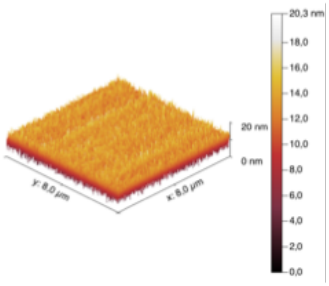
c) 3D AFM image of upper surface of the TO8-C2-3</td></tr>
<tr><td> 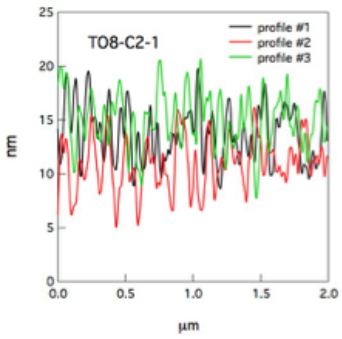

d) Typical height profiles of the TO8-C2-1</td><td> 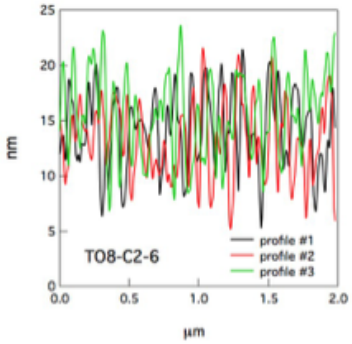

e) Typical height profiles of the TO8-C2-6</td><td> 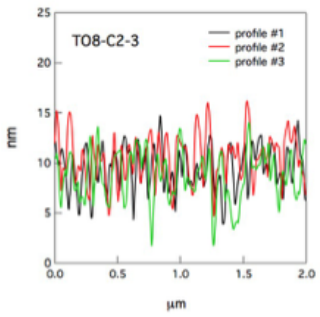

f) Typical height profiles of the TO8-C2-3</td></tr>
</table>

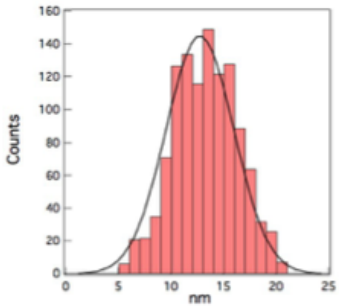

g) Histogram of the heights (red columns) and the fit (black line) of the TO8-C2-1.

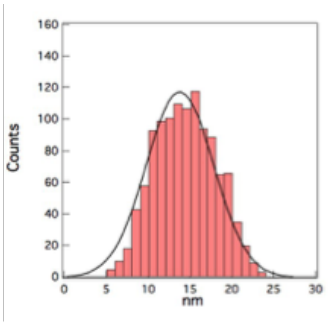

h) Histogram of the heights (red columns) and the fit (black line) of the TO8-C2-6.

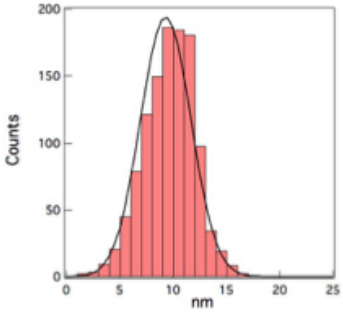

i) Histogram of the heights (red columns) and the fit (black line) of the TO8-C2-3

Fig. 14 – AFM data and analysis. Panels a, b, and c show the 3D images of the TO8-C2-1, TO8-C2-6, and TO8-C2-3, respectively. Panels d, e, and f show typical height profiles. Panels g, h, and i report the histograms of the above height profiles.

The roughness of the samples was calculated as reported:

$$R = \sqrt{\frac{1}{N}\sum_{j=1}^{N} r_j^2}$$

where rj is the difference between the height and the average height of the j-th measurement. The calculated roughness for the samples TO8-C2-1, TO8-C2-6, and TO8-C2-3 are 1.95 nm, 3.56 nm, and 2.39 nm, respectively. Among these samples, only the sample TO8-C2-3 has been irradiated, we can conclude that the roughness is not significantly affected by irradiation.

The height data, obtained from the z-profiles (figs. 14 d-e-f), are reported in three histogram plots (figs. 14 g-h-i) and fitted using a Gaussian curve. The average heights correspond to the maxima of the fits. The obtained average heights for the samples TO8-C2-1, TO8-C2-6, and TO8-C2-3 are 12.75 nm, 13.78 nm, and 9.32 nm, respectively.

The AFM analysis suggests that the average heights of the pristine samples are larger than the irradiated filter. One possible interpretation is that proton irradiation partially removes the surface aluminum. In order to confirm this, X-ray transmission measurements will be necessary to derive the total amount of aluminum on pristine and irradiated samples.

7. X-Ray Transmission Measurements and Analysis

The transmission model based on the imaginary part of the atomic scattering factors tabulated in the literature does not take into account fine structure features that occur near the absorption edges (XANES and EXAFS) of the atomic elements present in the filter materials. High spectral resolution transmission measurements over the 0.1 – 2.5 keV energy range are necessary to measure the mass attenuation coefficient, in the absorption edge regions of the atomic elements in the filter material.

X-ray transmission measurements are also necessary to derive layer thicknesses for each filter material and assess its spatial uniformity.

7.1 X-ray Transmission Model

The main purpose of this section is to explain the model of the transmission curve and how to derive the areal density of each material along with its corresponding thickness. Two fit functions were used, one involving single atoms (elements), disregarding the stoichiometry, and the other using directly filter materials. The fit with elements has up to 4 parameters corresponding to each atomic areal density:

$$T(E)_{filter(elements)} = T_{Al} * T_{Si} * T_O * T_N = e^{\left[-\frac{\mu}{\rho}(E)\rho x\right]_{Al}} * e^{\left[-\frac{\mu}{\rho}(E)\rho x\right]_{Si}} * e^{\left[-\frac{\mu}{\rho}(E)\rho x\right]_O} * e^{\left[-\frac{\mu}{\rho}(E)\rho x\right]_N}$$

Hydrogen was not included since it does not contribute to the filter transmission in the investigated energy range. From the areal density ρx_{Al} it is possible to approximately calculate the thickness of the Al layer by dividing it for the Al bulk density of 2.7 g/cm^3 (doing so one considers only the metallic aluminum).

To estimate the silicon nitride thickness, one can calculate the equivalent thickness of either the N or the Si layer (ideally the two values should coincide) within the SiN_y by using a stoichiometry y=4/3:

$$x_N = \frac{\rho x_N}{\rho_{SiN_y} f_N}$$

$$f_N = \frac{yA_N}{yA_N + A_{Si}}$$

where f_N is the fraction of nitrogen within the silicon nitride, calculated by dividing the total mass of N by the silicon nitride relative molecular mass.

The fit using materials has up to 3 parameters, each corresponding to a material thickness:

$$T(E)_{filter(materials)} = e^{\left[-\frac{\mu}{\rho}(E)\rho x\right]_{Al}} * e^{\left[-\frac{\mu}{\rho}(E)\rho x\right]_{Al2O3}} * e^{\left[-\frac{\mu}{\rho}(E)\rho x\right]_{Si3N4}}$$

Aluminum oxide was introduced as a material, since its presence is a well-established fact in the literature, and it was experimentally measured in our XPS campaign. The advantage of using materials instead of atoms lies in that it is possible to directly obtain each layer thickness (using the following densities: ρ_{Al} = 2.7 g/cm^3, ρ_{Al2O3} = 3.97 g/cm^3, ρ_{Si3N4} = 3.44 g/cm^3) and make a comparison with the nominal thicknesses quoted by the vendor.

Finally, a different equation needs to be introduced for filters with a mesh, which takes into account both the mesh open area (OA) and material, which is not necessarily opaque over the full energy range, and could become transparent to X-rays at the higher end of it. To this end, two more parameters are introduced to account for mesh material thickness and OA. It must be kept in mind that the OA is an "effective" value, and not the nominal one, meaning that it depends on the mesh portion sampled by the beam spot:

$$T(E)_{filter+mesh} = T(E)_{filter(materials)} * \left[OA + (1 - OA) * e^{\left[-\frac{\mu}{\rho}(E)\rho x \right]_{Si\_mesh}} \right]$$

If the beam spot size is comparable with the mesh pitch and its position on the sample changes during the measurement, as it occurs over an energy sweep, since the monochromator angle changes with energy and this in turns influences the beam spot position on the sample, it becomes very difficult to reconstruct the transmission curve.

7.2 Measurements at PTB-EUV and PTB-Xray beamlines of BESSY II

X-ray transmission measurements were performed in June 2019 at two BESSY II synchrotron beamlines on a group of filter samples produced by AMETEK made of a thin silicon nitride layer of either 40 nm or 145 nm, whose chemical composition is assumed to be Si_3N_4, coated with a thin Al layer of either 10 nm or 15 nm on each side. In some samples, a supporting Si mesh with a honeycomb pattern is present. The mesh is characterized by bar width, bar height (mesh thickness), cell pitch and by a resulting overall open area (OA) reported in the table in ANNEX1. Two of the measured samples underwent 10 MeV protons irradiation with a fluence equal to $1.2 \cdot 10^{10}$ protons/cm^2 (QF) and 10 times QF. The nominal thicknesses of the set of filters, along with their mesh parameters, are summarized in table 5.

Table 5: Nominal layer thicknesses for the Al/SiN/Al AMETEK filter samples measured at BESSY II.

Filters	Al (nm)	Si_3N_4 (nm)	Si mesh (µm)	OA (%)	Mesh features (µm)
LAOF-S1-C1B5-W1-F5	0	40±5%	-	-	-
LAOF-S1-C1B5-W2-F2	2x15±5%	40±5%	50±1	97	
TO8-C1-1	2x10±5%	145±5%	-	-	-
TO8-C2-6	2x15±5%	40±5%	15±1	82	bar width 17 pitch size 200
TO8-C2-5	2x15±5%	40±5%	15±1	82	bar width 17 pitch size 200
TO8-C2-2	2x15±5%	40±5%	15±1	82	bar width 17 pitch size 200
TO8-C2-31	0	40±5%	15±1	81	bar width 17 pitch size 200

Samples were measured at two X-ray beamlines of the Physikalisch Technische Bundesanstalt at BESSY II in Berlin – Germany, to obtain X-ray transmission measurements in both the soft energy range 50-1800 eV (PTB EUV beamline) and in the hard energy range 1750-3600 eV (PTB X-Ray beamline). The investigated energy ranges include edges of the elements present in the filter: Al L-edges @73 eV and @118 eV, Si L-edges @99 eV and @149 eV, N K-edge @402 eV, O K-edge @532 eV, Al K-edge @1560 eV and Si K-edge @1839 eV.

The use of both PTB beamlines at BESSY II was made available by ESA within the implementation of this research project. A brief description of the PTB beamlines is given in TN9.

The X-ray transmission measurements performed @PTB-EUV beamline on AMETEK filter samples were obtained in the energy range between 50 eV and 1800 eV, using different energy steps, as reported in table 6. Data near the C K-edge were not acquired since they were considered unreliable due to Carbon contamination of the chamber. The properties of the light spot for the PTB-EUV beamline at the sample surface were:

- light incidence and source: normal and bending magnet;
- spot size ~1.2 x 1.0 mm^2 (vertical x horizontal);
- spectral resolving power better than 1000.

Table 6: Energy steps adopted for the x-ray absorption spectroscopy at PTB EUV.

Absorption Edges		**Al-L**	**Si-L**		**N-K**		**O-K**		**Al-K**	
Energy range (eV)	50-70	70-94	94-180	180-390	390-450	450-520	520-570	570-1550	1550-1700	1700-1800
Filters	**Energy step in each range (eV)**									
LAOF-S1-C1B5-W1-F5	2	2	0.2	5	0.4	5	10	20	10	10
LAOF-S1-C1B5-W2-F2	2	0.2	0.2	5	0.4	5	0.4	20	1	10
TO8-C1-1	2	0.2	0.2	5	0.4	5	0.4	20	1	10
TO8-C2-6	2	0.2	0.2	5	0.4	5	0.4	20	1	10
TO8-C2-5	2	0.2	0.2	5	0.4	5	0.4	20	1	10
TO8-C2-2	2	2	0.2	5	0.4	5	10	20	10	10
TO8-C2-31	2	2	0.2	5	0.4	5	10	20	10	10

All Si_3N_4 samples were also measured @PTB X-Ray beamline to obtain the transmission curves in the energy range 1750 - 3600 eV, by using different energy steps, as reported in table 7. The properties of the light spot for the PTB-Xray beamline at the sample surface were:

- light incidence and source: normal and bending magnet;
- spot size ~ 0.3 x 0.3 mm2 (v x h);
- spectral resolving power 10000.

Table 7: Energy steps adopted for the x-ray absorption spectroscopy at PTB X-Ray.

Absorption Edges		**Si-K**		
Energy range (eV)	1750-1830	1830-1900	1900-2200	2200-3600
Filters	**Energy Step in each range (eV)**			
LAOF-S1-C1B5-W1-F5	10	1	10	50
LAOF-S1-C1B5-W2-F2	10	1	10	50
TO8-C1-1	10	1	10	50
TO8-C2-6	10	1	10	50
TO8-C2-5	10	1	10	50
TO8-C2-2	10	1	10	50
TO8-C2-31	10	1	10	50

Data taken at both beamlines were merged together to obtain transmission curves over the whole energy range 50 eV to 3600 eV. Two best fits, one using elements and one using materials, were obtained for all the filter samples. Regarding filters with a mesh, two additional fit parameters, mesh thickness and OA, were considered, except where the mesh cell pitch was big enough (OA = 97%) that the beam spot was entirely within it. Figure 15 reports the measured transmission spectra together with their best fit curves.

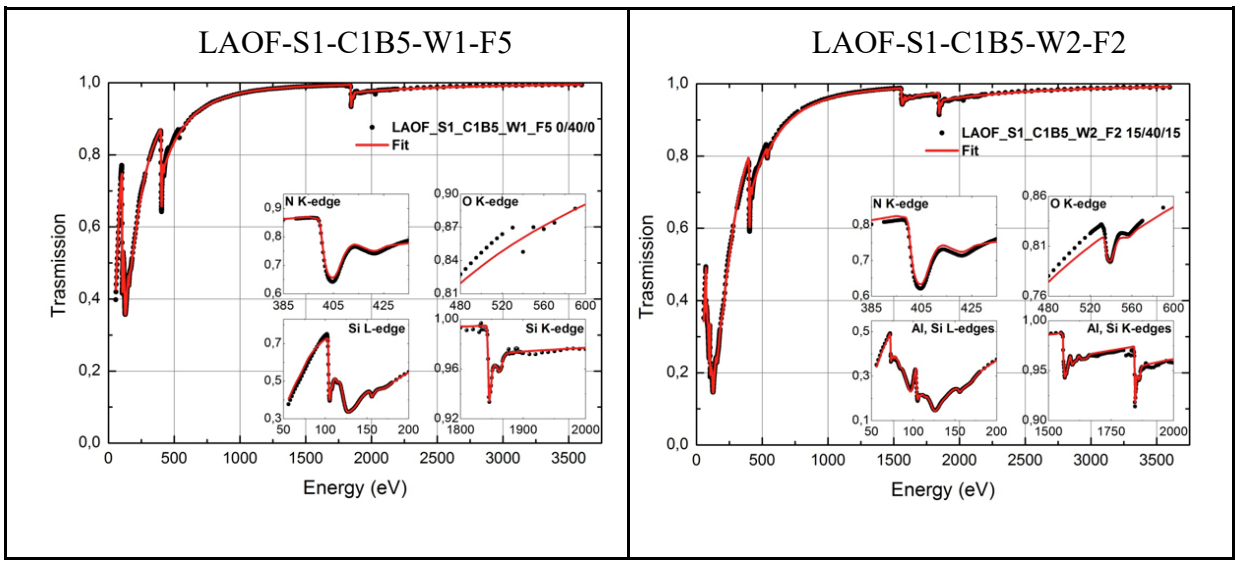

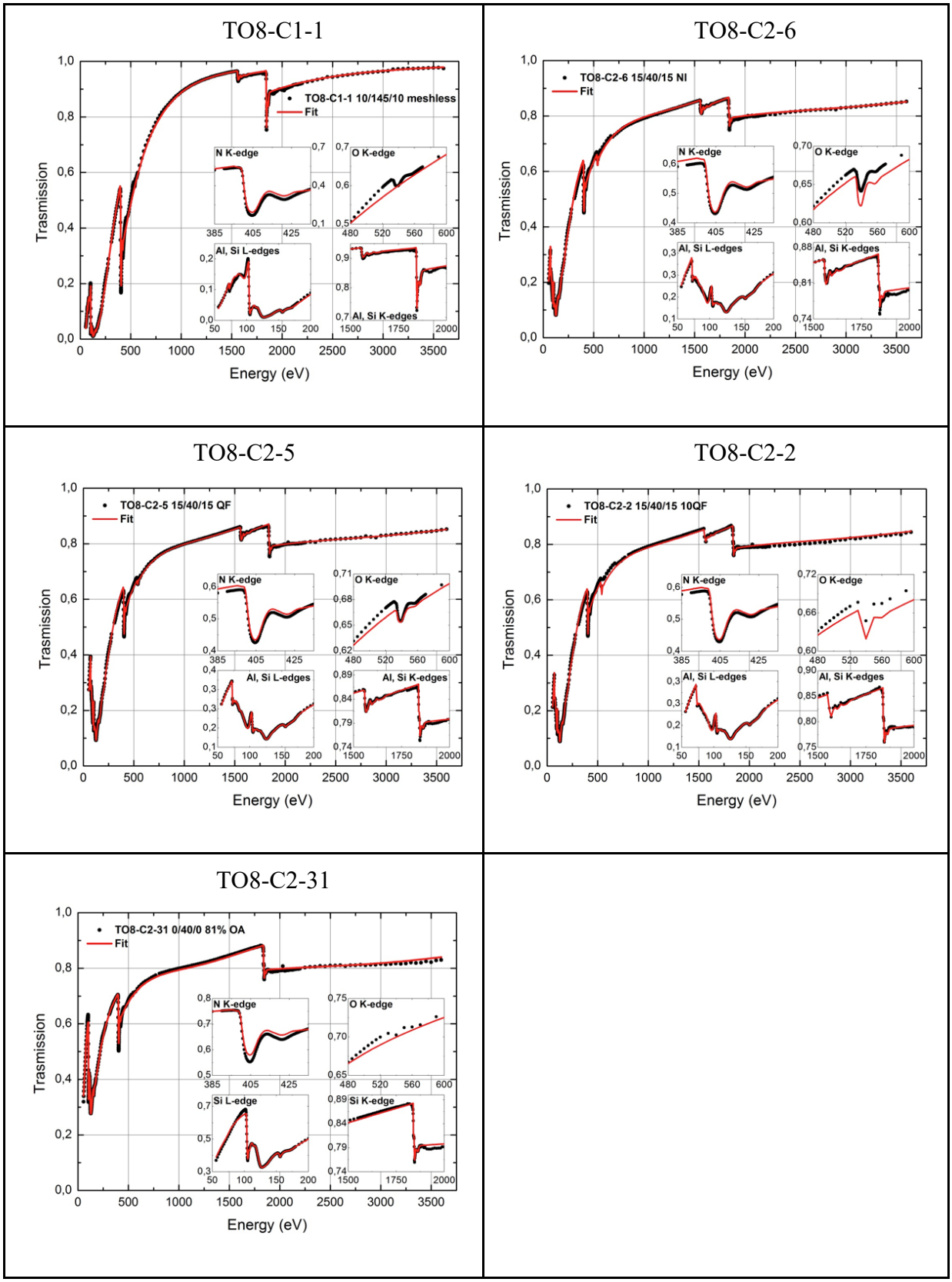

Fig. 15 - Experimental data (black points) of measured filters and the best fits on elements (red line).

The layer thicknesses, mesh thickness and OA obtained from the best fit on materials are reported in table 8, whereas the areal densities and OA obtained from the best fit on elements are summarized in table 9.

Table 8: Layer thickness of each material (Al, Al_2O_3, Si_3N_4, SiO_2, Si mesh) and open area (OA) with 3σ statistical uncertainty and nominal thickness for all filters, derived from a best fit analysis.

	Best fit thicknesses (nm)					**Nominal thicknesses (nm)**			
Filters	**Al**	**Si_3N_4**	**Al_2O_3**	**Si mesh (μm)**	**OA (%)**	**Al**	**Si_3N_4**	**Si mesh (μm)**	**OA (%)**
LAOF-S1-C1B5-W1-F5	-	36.9±0.1	-	-	-	-	40	-	-
LAOF-S1-C1B5-W2-F2	20.0±0.4	35.7±0.3	7.5±0.3	-	-	2x15	40	50	97
TO8-C1-1	17.9±1.6	142±1	2.5±1.3	-	-	2x10	145	-	-
TO8-C2-6	22.1±0.8	40.8±0.7	13.9±0.6	14.5±0.8	83.7±0.2	2x15	40	15	82
TO8-C2-5	26.3±0.5	38.6±0.5	6.9±0.4	13.4±0.5	83.3±0.2	2x15	40	15	82
TO8-C2-2	21±1	37.4±0.6	14.7±0.9	13.3±0.8	82.7±0.2	2x15	40	15	82
TO8-C2-31	-	38.5±0.2	-	13.3±0.9	81.5±0.2	-	40	15	81

Table 9: Areal densities of each element (Al, Si, O, N, Si mesh) and open area (OA) with 3σ statistical uncertainty, derived from a best fit analysis.

	Areal densities (10^{-7} g/cm^2)				***Thickness (μm)***	***(%)***
Filters	**Al**	**Si**	**O**	**N**	**Si mesh**	**OA**
LAOF-S1-C1B5-W1-F5	-	74.4±0.3	0±0.7	54.7±0.9	-	-
LAOF-S1-C1B5-W2-F2	72.0±0.6	70.1±0.7	9.8±0.7	54.5±0.7	-	-
TO8-C1-1	54±2	280±3	0±3	205±3	-	-
TO8-C2-6	94.1±1.4	75.3±1.5	18.2±1.2	66.4±1.4	34.1±1.5	83.9±0.2
TO8-C2-5	88.6±0.8	74±1	7.6±0.8	60±1	31.7±0.9	83.5±0.1
TO8-C2-2	92.2±1.4	69.9±1.4	21.5±1.5	58.4±1.2	31.6±1.6	82.9±0.2
TO8-C2-31	-	78.7±0.6	0±1	56.0±1.5	32±2	81.8±0.2

As can be seen from table 8, the sum of the Al and the Al_2O_3 thicknesses is in agreement, within the uncertainty, with the total amount of Al expected, although in most cases it is slightly overestimated. Furthermore, for the samples with the substrate in silicon nitride, the Al_2O_3 thickness varies from sample to sample, probably due to the fit being less accurate around the O K-edge. The silicon nitride is consistently underestimated except in one instance. Finally, as already stated, the OA effectively seen by the beam is different from the nominal one, since the beam spot size can hit any portion of the mesh (just a bar, no bars, two bars crossing). Estimating mesh thickness with any sort of precision is trickier because both the OA and the mesh areal density are interdependent parameters and difficult to disentangle for the optimization algorithm. On top of that, the beam spot moves over the sample surface as energies are scanned, hitting different parts of the mesh.

From table 9, the equivalent thicknesses of the Al layer are in agreement with those found using the fit on materials. The silicon nitride thicknesses calculated from N areal densities are in agreement with the nominal ones, except for the samples supported by the mesh, whereas those calculated from Si are consistently underestimated by a few nm. Figure 15 reports the measured transmission spectra together with their best fit curves. Two noticeable features are: thinner (40 nm of SiN) filters have more Al oxide than the thicker one (145 nm of SiN) and filters without Al still have some oxygen atoms, probably due to either Si oxidation or water molecules/OH groups adhering to the membrane surface.

7.3 Measurements at the BEAR beamline of ELETTRA

An x-ray transmission measurements campaign was performed in November-December 2019 at the BEAR beamline of ELETTRA on three CNT small samples mounted on TF111 standard frames, produced by AMETEK, and on two samples Polyimide/Al with polyimide mesh, produced by Oxford. Nominal thicknesses for both sets of filters, along with their mesh parameters, are summarized in table 10 and table 11.

Table 10: Nominal layer thicknesses for the Al/SiN/Al filters samples measured at ELETTRA.

Filters	Al (nm)	CNT (nm)
LAOF-CNT2-C1B3-F18 (68)	-	210-270
LAOF-CNT2-C1B3-F19 (69)	14 x 2	210-270
LAOF-CNT2-C1B2-F02 (52)	14 x 2	120-150

Table 11: Nominal layer thicknesses for the Al/Polyimide/Al filters samples measured at ELETTRA.

Filters	Al (nm)	PI (nm)	PI mesh (µm)	OA (%)	Mesh features (µm)
OIT-TF111-80	15 x 2	55	18	97	PI S2b bar width=10 um, pitch=652 um
OIT-TF111-81	15 x 2	55	18	97	PI S2b bar width=15 um, pitch=977 um

Samples were measured at the BEAR beamline at ELETTRA synchrotron in Trieste – Italy to obtain X-ray transmission measurements in the energy range 40-1650 eV by using the G1200 monochromator. The energy range investigated includes the following edges of the elements present in the filter: Al L-edges @73 eV and @118 eV, Si L-edges @99 eV and @149 eV, N K-edge @402 eV, O K-edge @532 eV, Al K-edge @1560 eV. A brief description of the BEAR beamline is given in TN9. The properties of the light spot at the sample surface were:

- light incidence and source: normal and bending magnet;
- spot size ~400 um x 50 um (vertical x horizontal)

The energy range and relative filter used in G1200 monochromator were:

- 40-75 eV Al
- 70-104 eV Si
- 100-180 eV no filter
- 176-260 eV no filter
- 250-330 eV Ag
- 310-600 eV no filter
- 550-1000 eV no filter
- 900-1600 eV Ag

The X-ray transmission measurements performed @BEAR beamline were obtained in the energy range between 40 eV and 1650 eV, using different energy steps, as reported in table 12.

Table 12: Energy steps adopted for the x-ray absorption spectroscopy at the BEAR beamline of ELETTRA.

Absorption Edges		**Al-L**				**C-K**		**N-K**		**O-K**				**Al-K**
Energy range (eV)	40-75	70-104	100-80	176-260	250-285	280-340	340-390	390-450	450-520	510-560	560-600	550-950	900-1440	1440-1650
Filters	**Energy range used in each step (eV)**													
LAOF-CNT2-C1B3-F18	2	2	2	2	2	0.1	2	0.1	2	0.1	10	10	10	1
LAOF-CNT2-C1B3-F19	2	0.1	2	2	2	0.1	2	0.1	2	0.1	10	10	10	1
LAOF-CNT2-C1B2-F02	2	0.1	2	2	2	0.1	2	0.1	2	0.1	10	10	10	1
OIT-TF111-80	2	0.1	2	2	2	0.1	2	0.1	2	0.1	10	10	10	1
OIT-TF111-81	2	0.1	2	2	2	0.1	2	0.1	2	0.1	10	10	10	1